A Structural and Spectroscopic Characterization of $[Pt_3(PPh_3)_3(\mu\text{-}PPh_2)_2(\mu\text{-}H)][BF_4]\cdot 2CH_2Cl_2$ †

By **Pier Luigi Bellon,* Alessandro Ceriotti, Francesco Demartin,** and **Giuliano Longoni,*** Istituto di Chimica Generale e Centro del C.N.R., via Venezian 21, 20133 Milano, Italy
Brian T. Heaton,* Chemical Laboratory, University of Kent, Canterbury CT2 7NH

The previously reported cationic cluster $[Pt_3(PPh_3)_4]^+$ has been shown to be $[Pt_3(PPh_3)_3(\mu\text{-}PPh_2)_2(\mu\text{-}H)]^+$ by *X*-ray structural analysis and ^{31}P n.m.r. studies. The presence of a bridging hydride ligand could not be detected in the *X*-ray structural determination nor by direct ^1H n.m.r. studies, but was unambiguously established by ^{31}P and $^{31}P\text{-}\{^1H\}$ n.m.r. measurements at 145.8 MHz.

SEVERAL triangular neutral and cationic transition-metal cluster compounds stabilized by phosphine ligands are now known.[1-6] Our interest in this class of compounds led us to reinvestigate a platinum cluster reported some years ago [7] and tentatively formulated as $[Pt_3(PPh_3)_4]^+$ on the basis of analytical data.

The compound has been synthesized as previously reported; [7] an *X*-ray structural determination on a golden-yellow needle grown from dichloromethane, combined with ^{31}P n.m.r. measurements, shows that this compound must be reformulated as $[Pt_3(PPh_3)_3(\mu\text{-}PPh_2)_2(\mu\text{-}H)][BF_4]\cdot 2CH_2Cl_2$ (1).

EXPERIMENTAL

The compound $[Pt_3(PPh_3)_3(\mu\text{-}PPh_2)_2(\mu\text{-}H)][BF_4]\cdot 2CH_2Cl_2$ was prepared by u.v. irradiation of an ethanolic solution of $[Pt(PPh_3)_2(C_2O_4)]$ under a hydrogen atmosphere, followed by precipitation with $Na[BF_4]$ in water and crystallization from dichloromethane and n-heptane, as previously reported for $[Pt_3(PPh_3)_4][BF_4]$ [7] (Found: C, 49.2; H, 3.5; Pt, 29.8. Calc. for $C_{80}H_{70}BCl_4F_4P_5Pt_3$: C, 48.0; H, 3.5; Pt, 29.3%). The compound shows i.r. absorptions (Nujol mull) at 3 050w, 1 590w, 1 570w, 1 480m, 1 435s, 1 310w, 1 275w, 1 225w, 1 185w, 1 160w, 1 100s, 1 060s, 1 030(sh), 1 000mw, 740s, 730m, and 690s cm^{-1}.

Attempts were made to collect ^1H n.m.r. spectra on a Fourier-transform JEOL PS-100 spectrometer using 5-mm n.m.r. tubes containing *ca.* 0.1 mol dm^{-3} solutions but, after typically 50 000 scans, nothing was observed in the high-field region. Phosphorus-31 n.m.r. spectra were measured on a Bruker WH360 spectrometer at 145.8 MHz using 10-mm n.m.r. tubes. A sweepwidth of 45 kHz was used with 32K computer points (digital resolution 2.8 Hz). The spectra were referenced to external H_3PO_4 (0.05 mol dm^{-3}) in D_2O.

Crystal Data.—$C_{80}H_{70}BCl_4F_4P_5Pt_3$, $M = 2\,000.2$, Triclinic, space group $P\bar{1}$ (C_i^1, no. 2), $a = 20.799(6)$, $b = 15.029(5)$, $c = 13.822(4)$ Å, $\alpha = 111.08(2)$, $\beta = 73.89(3)$, $\gamma = 102.87(3)°$, $U = 3\,836.5$ Å^3, $D_m = 1.73$ g cm^{-3} (by flotation), $Z = 2$, $D_c = 1.730$ g cm^{-3} $F(000) = 1\,936$, μ(Mo-K_α) 60.4 cm^{-1}.

The cell parameters were obtained from least-squares refinement of 40 reflections accurately measured with graphite-monochromatized Mo-K_α radiation ($\lambda = 0.710\,73$ Å). The crystal was an oblique prism (0.21 × 0.13 × 0.46 mm) which was covered with a thin layer of polymeric acrylonitrile to avoid rapid decomposition by evaporation of the clathrated solvent.

Intensity data were collected on a BASIC diffractometer,[8] in the range θ 3—25°. Solution and refinement of the structure were based upon a set of 6 627 reflections (out of 8 094 independent measurements) having $I/\sigma(I) \geqslant 3$, which were corrected for Lorentz polarization and absorption effects.

The structure was solved by inspection of the Patterson map, which allowed the positions of the three platinum atoms to be assigned; subsequent Fourier syntheses displayed all the non-hydrogen atoms. Refinement by full-matrix least squares led finally to $R = 0.0345$ and $R' = [\Sigma w(F_o - k|F_c|)^2/wF_o^2]^{\frac{1}{2}} = 0.0410$. All observations were assigned with individual weights according to the equation $w_{hkl} = 1/[26.2 - 0.271\,kF_o + 0.0015(kF_o)^2]$.

The Pt, Cl, F, and P atoms were treated anisotropically, and phenyl rings were constrained to D_{6h} symmetry (C–C 1.392 Å); the total number of refined parameters was **313**. The contributions of the scattering amplitudes of all carbon-bonded hydrogen atoms, in their expected positions, were included in the computations. Form factors [9,10] and real and imaginary dispersion corrections [11] were used. A set of three difference-Fourier syntheses were finally computed to test whether a signal attributable to the hydridic hydrogen atom was present; the syntheses were computed at increasing values of limiting $(\sin^2\theta)/\lambda^2$ (0.09, 0.18, and 0.36).

TABLE 1

Positional parameters ($\times 10^4$) in $[Pt_3(PPh_3)_3(\mu\text{-}PPh_2)_2(\mu\text{-}H)][BF_4]\cdot 2CH_2Cl_2$

Atom	*x*	*y*	*z*
Pt(1)	2 220(0)	1 872(0)	−1 094(0)
Pt(2)	1 641(0)	2 563(0)	1 073(0)
Pt(3)	2 409(0)	1 189(0)	425(0)
P(1)	2 519(1)	2 004(2)	−2 773(2)
P(2)	1 037(1)	3 410(2)	2 625(2)
P(3)	2 848(1)	390(2)	1 124(2)
P(4)	1 426(1)	2 918(1)	−221(1)
P(5)	2 845(1)	708(1)	−1 301(2)
F(1)	2 218(5)	7 168(8)	3 834(8)
F(2)	2 606(6)	5 929(9)	2 505(10)
F(3)	3 046(7)	7 365(10)	2 516(12)
F(4)	3 247(6)	6 871(13)	3 604(11)
Cl(1)	4 237(4)	5 940(5)	−4 990(7)
Cl(2)	4 572(3)	7 916(5)	−4 725(6)
Cl(3)	4 682(3)	5 087(5)	1 560(6)
Cl(4)	3 490(3)	3 976(3)	751(4)
C(1)	4 445(12)	6 799(17)	−5 621(19)
C(2)	3 923(14)	5 129(19)	1 293(21)
B	2 754(10)	6 795(14)	3 182(15)

† 1,2;1,3-Bis(μ-diphenylphosphido)-2,3-μ-hydrido-*cyclo*-tris[(triphenylphosphine)platinum] tetrafluoroborate–dichloromethane (1/2).

TABLE 1 (*continued*)

Atom	*x*	*y*	*z*
C(111)	1 807(3)	2 003(7)	−3 321(6)
C(112)	1 189(4)	1 485(6)	−3 008(6)
C(113)	637(3)	1 459(6)	−3 408(6)
C(114)	705(3)	1 950(7)	−4 121(6)
C(115)	1 324(4)	2 469(6)	−4 434(6)
C(116)	1 875(3)	2 495(6)	−4 034(6)
C(121)	2 955(4)	1 049(5)	−3 853(5)
C(122)	2 599(2)	294(6)	−4 520(6)
C(123)	2 931(4)	−445(4)	−5 297(5)
C(124)	3 619(4)	−431(5)	−5 406(5)
C(125)	3 975(2)	323(6)	−4 738(6)
C(126)	3 643(4)	1 063(4)	−3 962(5)
C(131)	3 103(5)	3 092(5)	−2 817(6)
C(132)	3 183(4)	3 808(5)	−1 867(4)
C(133)	3 599(4)	4 671(4)	−1 879(5)
C(134)	3 934(5)	4 817(5)	−2 843(6)
C(135)	3 855(4)	4 101(5)	−3 794(4)
C(136)	3 439(4)	3 239(4)	−3 781(5)
C(211)	643(4)	4 385(4)	2 631(6)
C(212)	107(4)	4 117(4)	2 120(6)
C(213)	−181(3)	4 818(5)	2 012(6)
C(214)	66(4)	5 787(4)	2 415(6)
C(215)	602(4)	6 055(4)	2 926(6)
C(216)	891(3)	5 354(5)	3 034(6)
C(221)	314(4)	2 639(5)	3 145(6)
C(222)	−215(4)	3 014(4)	3 963(7)
C(223)	−750(3)	2 397(5)	4 340(5)
C(224)	−756(4)	1 405(5)	3 900(6)
C(225)	−226(4)	1 030(4)	3 082(7)
C(226)	308(3)	1 646(5)	2 704(5)
C(231)	1 520(4)	3 971(7)	3 679(5)
C(232)	1 212(3)	4 468(7)	4 709(6)
C(233)	1 590(4)	4 892(4)	5 488(4)
C(234)	2 276(4)	4 819(7)	5 237(5)
C(235)	2 584(3)	4 322(7)	4 207(6)
C(236)	2 206(4)	3 898(4)	3 427(4)
C(311)	2 224(3)	−181(6)	2 027(6)
C(312)	1 712(4)	336(4)	2 733(7)
C(313)	1 228(4)	−61(6)	3 442(6)
C(314)	1 255(3)	−977(6)	3 444(6)
C(315)	1 767(4)	−1 495(4)	2 738(7)
C(316)	2 251(4)	−1 097(6)	2 030(6)
C(321)	3 409(4)	1 226(5)	1 954(5)
C(322)	3 525(4)	1 037(4)	2 802(6)
C(323)	3 965(3)	1 684(6)	3 412(5)
C(324)	4 289(4)	2 520(5)	3 174(5)
C(325)	4 174(4)	2 709(4)	2 327(6)
C(326)	3 733(3)	2 062(6)	1 717(5)
C(331)	3 336(4)	−587(5)	238(5)
C(332)	4 001(4)	−575(4)	267(5)
C(333)	4 358(3)	−1 320(6)	−435(6)
C(334)	4 050(4)	−2 077(5)	−1 167(5)
C(335)	3 385(4)	−2 090(4)	−1 197(5)
C(336)	3 027(3)	−1 345(6)	−494(6)
C(411)	574(3)	2 431(5)	−429(7)
C(412)	144(4)	2 972(4)	−518(7)
C(413)	−507(4)	2 558(5)	−651(7)
C(414)	−728(3)	1 602(5)	−694(7)
C(415)	−297(4)	1 061(4)	−604(7)
C(416)	353(4)	1 475(5)	−472(7)
C(421)	1 613(5)	4 121(4)	−314(5)
C(422)	1 551(4)	4 285(4)	−1 211(5)
C(423)	1 768(4)	5 194(4)	−1 328(4)
C(424)	2 045(5)	5 938(4)	−547(5)
C(425)	2 106(4)	5 774(4)	349(5)
C(426)	1 890(4)	4 865(4)	466(4)
C(511)	2 533(4)	−490(4)	−2 063(6)
C(512)	1 894(4)	−866(4)	−1 607(4)
C(513)	1 606(3)	1 785(6)	−2 126(6)
C(514)	1 956(4)	−2 328(4)	−3 099(6)
C(515)	2 595(4)	−1 952(4)	−3 554(4)
C(516)	2 884(3)	−1 033(6)	−3 036(6)
C(521)	3 762(2)	908(5)	−1 647(7)
C(522)	4 062(4)	1 861(5)	−1 482(7)
C(523)	4 762(4)	2 083(4)	−1 656(7)
C(524)	5 162(2)	1 353(5)	−1 993(7)
C(525)	4 862(4)	400(5)	−2 159(7)
C(526)	4 162(4)	178(4)	−1 985(7)

A peak was detected in all syntheses, essentially at the midpoint of vector Pt(2)–Pt(3) with heights 0.50, 0.70, and 0.97 respectively. These peaks, however, must be due to a residual contribution of metal atoms since they are higher than expected for a hydrogen atom,[12] and the distances from the platinum atoms (1.3—1.4 Å) are not sound for a Pt–H interaction. Table 1 lists the final atomic co-ordinates for non-hydrogen atoms. Thermal parameters and a list of computed and observed structure factors are available as Supplementary Publication No. SUP 23313 (28 pp.).*

TABLE 2

Selected intramolecular distances (Å) and angles (°) in $[Pt_3(PPh_3)_3(\mu\text{-}PPh_2)_2(\mu\text{-}H)][BF_4]\cdot 2CH_2Cl_2$

(*a*) Within the Pt_3P_5 moiety

Pt(1)–Pt(2)	2.796(1)	Pt(1)–Pt(2)–P(2)	161.4(1)
Pt(1)–Pt(3)	2.795(1)	Pt(3)–Pt(2)–P(2)	136.8(1)
Pt(2)–Pt(3)	2.638(1)	Pt(1)–Pt(3)–P(3)	158.8(1)
Pt(1)–P(1)	2.299(3)	Pt(2)–Pt(3)–P(3)	138.9(1)
Pt(2)–P(2)	2.248(2)	Pt(1)–Pt(2)–P(4)	53.4(1)
Pt(3)–P(3)	2.241(4)	Pt(2)–Pt(1)–P(4)	50.4(1)
Pt(1)–P(4)	2.312(3)	Pt(1)–Pt(3)–P(5)	53.1(1)
Pt(2)–P(4)	2.220(3)	Pt(3)–Pt(1)–P(5)	50.3(1)
Pt(1)–P(5)	2.299(3)	Pt(1)–P(4)–Pt(2)	76.2(1)
Pt(3)–P(5)	2.212(2)	Pt(1)–P(5)–Pt(3)	76.6(1)
Pt(2)–Pt(1)–Pt(3)	56.3(1)	P(1)–Pt(1)–P(4)	102.6(1)
Pt(1)–Pt(2)–Pt(3)	61.8(1)	P(1)–Pt(1)–P(5)	101.1(1)
Pt(1)–Pt(3)–Pt(2)	61.9(1)	P(4)–Pt(1)–P(5)	156.1(1)
Pt(2)–Pt(1)–P(1)	151.3(1)	P(2)–Pt(2)–P(4)	108.1(1)
Pt(3)–Pt(1)–P(1)	150.7(1)	P(3)–Pt(3)–P(5)	105.9(1)

(*b*) Within the ligands

P(1)–C(111)	1.841(10)	P(3)–C(321)	1.819(8)
P(1)–C(121)	1.844(7)	P(3)–C(331)	1.836(8)
P(1)–C(131)	1.816(8)	P(4)–C(411)	1.818(8)
P(2)–C(211)	1.828(10)	P(4)–C(421)	1.806(7)
P(2)–C(221)	1.828(8)	P(5)–C(511)	1.809(7)
P(2)–C(231)	1.841(9)	P(5)–C(521)	1.814(6)
P(3)–C(311)	1.832(8)		
		Pt(1)–P(1)–C(111)	114.8(3)
Pt(1)–P(1)–C(121)	117.6(3)	Pt(1)–P(4)–C(411)	115.3(3)
Pt(1)–P(1)–C(131)	111.4(3)	Pt(1)–P(4)–C(421)	114.4(3)
Pt(2)–P(2)–C(211)	118.0(3)	Pt(2)–P(4)–C(411)	112.7(4)
Pt(2)–P(2)–C(221)	111.1(2)	Pt(2)–P(4)–C(421)	122.7(3)
Pt(2)–P(2)–C(231)	113.6(3)	Pt(1)–P(5)–C(511)	114.2(4)
Pt(3)–P(3)–C(311)	114.3(3)	Pt(1)–P(5)–C(521)	121.1(3)
Pt(3)–P(3)–C(321)	109.8(4)	Pt(3)–P(5)–C(511)	117.2(3)
Pt(3)–P(3)–C(331)	119.4(3)	Pt(3)–P(5)–C(521)	114.3(3)

(*c*) Within the BF_4^- anion

B–F(1)	1.314(22)	F(1)–B–F(2)	113.3(16)
B–F(2)	1.330(21)	F(2)–B–F(3)	103.2(16)
B–F(3)	1.406(29)	F(3)–B–F(4)	100.7(16)
B–F(4)	1.278(29)	F(1)–B–F(4)	115.8(16)
B–F(mean)	1.332(54)		

(*d*) Within the solvent molecules

C(1)–Cl(1)	1.722(31)	C(2)–Cl(4)	1.767(26)
C(1)–Cl(2)	1.706(22)	Cl(1)–C(1)–Cl(2)	109.9(15)
C(2)–Cl(3)	1.737(35)	Cl(3)–C(2)–Cl(4)	113.1(18)

RESULTS AND DISCUSSION

X-Ray Crystallographic Analysis.—The crystal structure of $[Pt_3(PPh_3)_3(\mu\text{-}PPh_2)_2(\mu\text{-}H)][BF_4]\cdot 2CH_2Cl_2$ (**1**) consists of an ionic packing in space group $P\bar{1}$ (Figure 1), which seems to be predominantly dictated by van der Waals interactions between the bulky $[Pt_3(PPh_3)_3(\mu\text{-}PPh_2)_2(\mu\text{-}H)]^+$ cations. The cavities between cations

* For details see Notices to Authors No. 7, *J. Chem. Soc., Dalton Trans.*, 1981, Index issue.

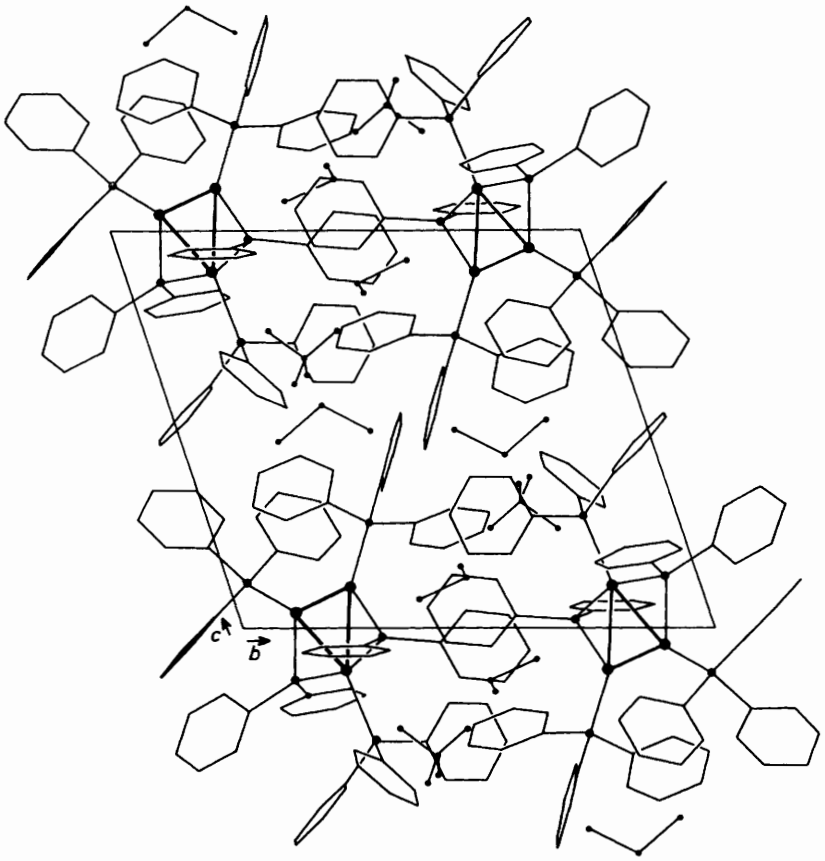

FIGURE 1 The crystal packing along the *a* axis

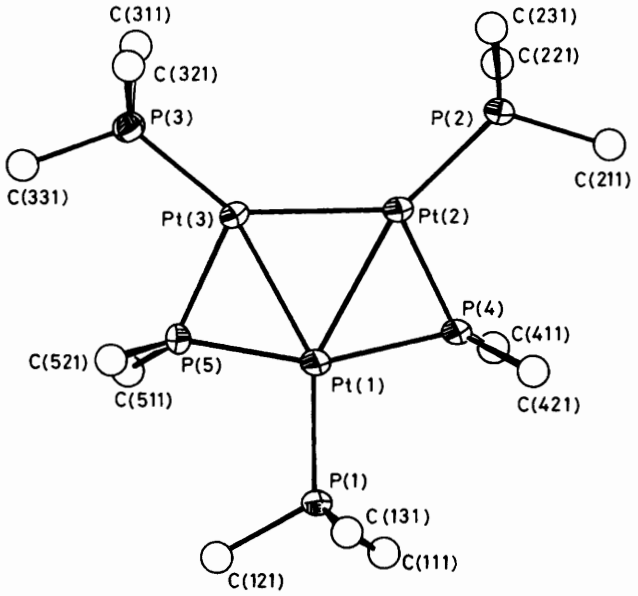

FIGURE 2 View of the cation $[Pt_3(PPh_3)_3(\mu\text{-}PPh_2)_2(\mu\text{-}H)]^+$ projected onto the plane of the Pt_3 triangle. The bridging hydride is not represented and only the first carbon atom of each phenyl ring is shown

TABLE 3

Planes through selected groups of atoms

(*a*) Equations of planes in the form $ax + by + cz + d = 0$ with deviations (Å) of atoms from planes in square brackets

	a	*b*	*c*	*d*
Plane 1: Pt(1), Pt(2), Pt(3)				
[P(1) 0.2857(3), P(2) −0.0156(3), P(3) 0.1552(3), P(4) −0.2535(2), P(5) 0.0156(2), C(411) −1.9271(7), C(421) 0.9275(8), C(511) −1.4815(8), C(521) 1.4814(6)]				
	14.9262	7.6016	1.5574	−4.5686
Plane 2: Pt(1), Pt(2), P(4)				
[C(411) −1.5561(7), C(421) 1.3633(8)]				
	12.8145	9.3689	0.4333	−4.5520
Plane 3: Pt(1), Pt(3), P(5)				
[C(511) −1.5059(8), C(521) 1.4565(6)]				
	14.8255	7.6823	1.6022	−4.5547
Plane 4: P(4), C(411), C(421)				
	3.6284	−9.4510	−11.4538	−0.3474
Plane 5: P(5), C(511), C(521)				
	−7.0670	10.0383	−12.9071	−0.3797

(*b*) Angles (°) between selected couples of planes

Plane	2	3	4	5
1	8.2	0.5	−87.3	85.7
2			−87.4	
3				85.7

are occupied by the comparatively small $[BF_4]^-$ anions and two crystallographically independent molecules of CH_2Cl_2; the latter has a relatively high vapour pressure, and it has been necessary to lacquer the crystal, before

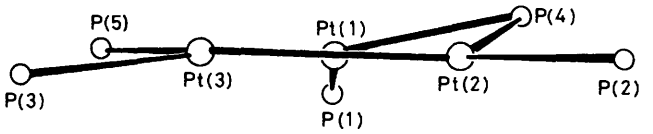

FIGURE 3 Projection of the Pt_3P_5 group onto a plane orthogonal to the Pt_3 triangle

exposure to air, in order to avoid rapid decay. Figure 2 shows the core of the $[Pt_3(PPh_3)_3(\mu\text{-}PPh_2)_2(\mu\text{-}H)]^+$ cation projected onto the plane of the Pt_3 triangle; the bridging hydrogen atom is omitted from the Figure since *X*-ray analysis could not establish its presence. However, subsequent high-field ^{31}P n.m.r. studies unambiguously showed the Pt(2)–Pt(3) edge to be H-bridged.

A collection of the most significant interatomic distances and angles is given in Table 2. The Pt_3P_5 moiety has C_{2v} symmetry (Figure 2) with the two-fold axis aligned with the P(1)–Pt(1) bond. However, there are strong deviations from planarity as can be seen in Table 3 and Figure 3. These distortions result essentially from ligand crowding in the proximity of the metal-atom triangle. It is of interest to compare (1) with previous structurally characterized compounds containing a triplatinum ring, *e.g.* $[Pt_3(Bu^tNC)_3(\mu\text{-}Bu^tNC)_3]$ (2)[13] $[Pt_3(PBu^t_3)_3(\mu\text{-}CO)_3]$ (3),[14] $[Pt_3\{P(C_6H_{11})_3\}_4(\mu\text{-}CO)_3]$ (4),[15] $[Pt_3Ph(PPh_3)_2(\mu\text{-}PPh_2)_3]$ (5),[1] and $[Pt_3(\mu\text{-}Ph)(PPh_3)_3(\mu\text{-}PPh_2)(\mu\text{-}SO_2)]$ (6).[4]

An understanding of the different Pt–Pt bond lengths in these triplatinum rings requires consideration of the number of valence electrons (v.e.) and the steric crowding brought about by bulky edge-bridging ligands. Uncrowded species with 42 v.e., such as (2) and (3), exhibit Pt–Pt bond distances in the range 2.63—2.65 Å whereas addition of a further pair of electrons (4) results in lengthening of the two edges involving the unique

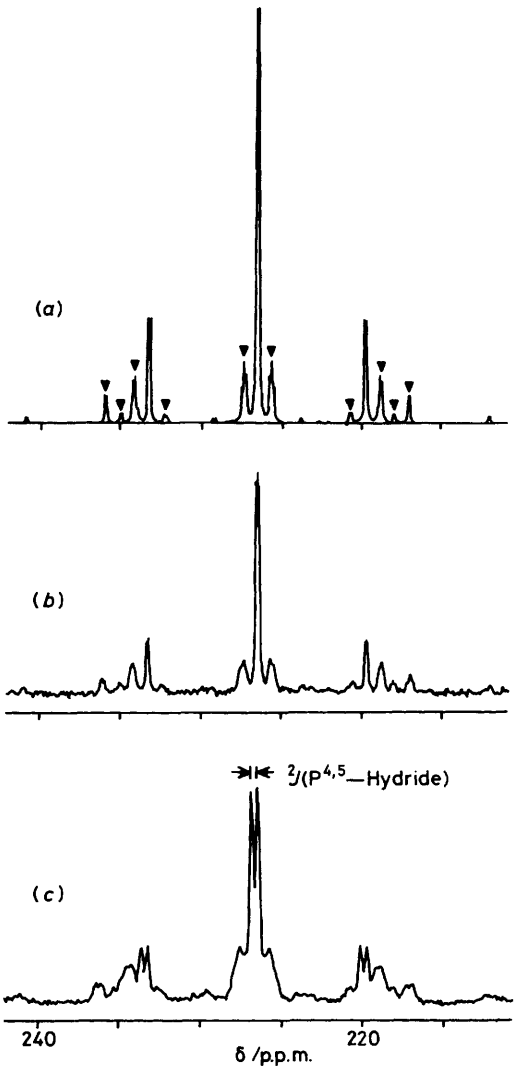

FIGURE 4 ^{31}P N.m.r. resonance due to the PPh_2 groups, $P^{4,5}$ (Figure 7), in $[Pt_3(PPh_3)_3(\mu\text{-}PPh_2)_2(\mu\text{-}H)]^+$: (*a*) simulated $^{31}P\text{-}\{^1H\}$ using the parameters in Table 4, (*b*) observed $^{31}P\text{-}\{^1H\}$, and (*c*) observed ^{31}P without ^1H decoupling. ▼, Peaks broadened due to P coupling to Pt^2 and/or Pt^3

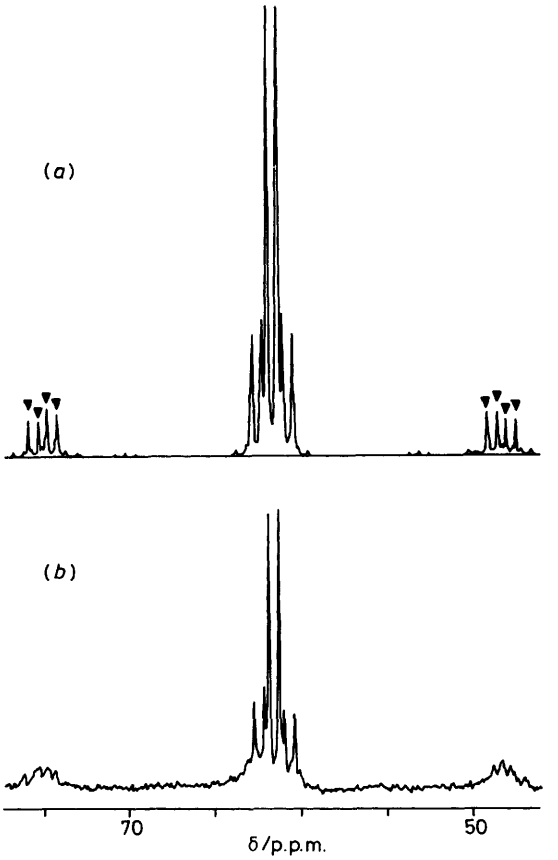

FIGURE 5 $^{31}P\text{-}\{^1H\}$ N.m.r. resonance due to the chemically equivalent PPh_2 groups, $P^{2,3}$ (Figure 7), in $[Pt_3(PPh_3)_3(\mu\text{-}PPh_2)_2(\mu\text{-}H)]^+$: (*a*) simulated using the parameters in Table 4 and (*b*) observed. ▼, Peaks broadened due to P coupling to Pt^2 and/or Pt^3

platinum (2.725 Å). In the highly crowded 44 v.e. species (5), two Pt–Pt bond distances, to the unique platinum, are 2.785 Å while the third is 3.65 Å; the latter is definitely non-bonding. Compounds (4) and (5), when compared with (2) and (3), suggest that the highest occupied molecular orbital (h.o.m.o.) in 44 v.e. Pt_3 clusters might be antibonding with respect to the Pt_3 triangle. Accordingly, the loss of two valence electrons on going from (5) to (1) results in ring closure. The PPh_2-bridged Pt–Pt bonds in (1) [Pt(1)–Pt(2) 2.796(1), Pt(1)–Pt(3) 2.795(1) Å] and in (5) are strictly comparable, whereas the H-bridged Pt(2)–Pt(3) bond [2.638(1) Å] has a length very similar to that found in the non-crowded 42 v.e. species (2) and (3). With regard to the length of Pt–P bonds, differences are noticed which depend more upon the particular metal atom than upon the type of ligand involved. So, barely noticeable differences exist among the three bonds involving Pt(1) [one toward the terminal P(1) and two toward the bridging P(4) and P(5) atoms], which range from 2.299(3) to 2.312(3) Å. The same is true for bonds Pt(2,3)–P(2,5), which exhibit lengths in the range 2.212(2)—2.248(2) Å. The longer distances observed for Pt(1)–P interactions can be due to either electronic or steric crowding of ligands in the vicinity of Pt(1).

^{31}P *N.M.R. Spectra.*—As originally reported,[7] (1) is diamagnetic and we have confirmed that it does not give a high-field hydride resonance in the 100-MHz n.m.r. spectra over a wide range of temperatures, even when using long (50 000 scans) collection times in either protio- or deuterio-solvents. This probably arises because of the complex spin system and similar low signal-to-noise ^{31}P and ^{195}Pt n.m.r. spectra were obtained at 45 and 21.4 MHz respectively. The presence of a bridging hydride ligand was only unambiguously established by obtaining ^{31}P and ^{31}P-{^1H} n.m.r. spectra at 145.8 MHz.

The observed ^{31}P-{^1H} n.m.r. spectra of (1) clearly show three kinds of phosphorus resonances due to the bridging phosphido-groups, P^4 and P^5, and to the two different types of triphenylphosphines, P^2 and P^3, and P^1 (see Figures 4, 5, and 6 respectively and Figure 1).* The PPh_2 resonance occurs at considerably higher frequency than the PPh_3 resonances and a detailed interpretation of the observed spectra requires consideration of five of the six isotopomers shown in Figure 7; isotopomer F can be neglected in the simulation because of its low probability and complex spin system, which gives rise to many lines of low intensity. The spectra have been simulated using the chemical shifts and coupling constants summarized in Table 4. All these values are close to those previously reported for $[Pd_3(PEt_3)_3(\mu\text{-}PPh_2)_2(\mu\text{-}Cl)]^+$ (7) [3] except for $^3J(P^2\text{–}P^3)$ which is twice the corresponding value found in (7). This probably results

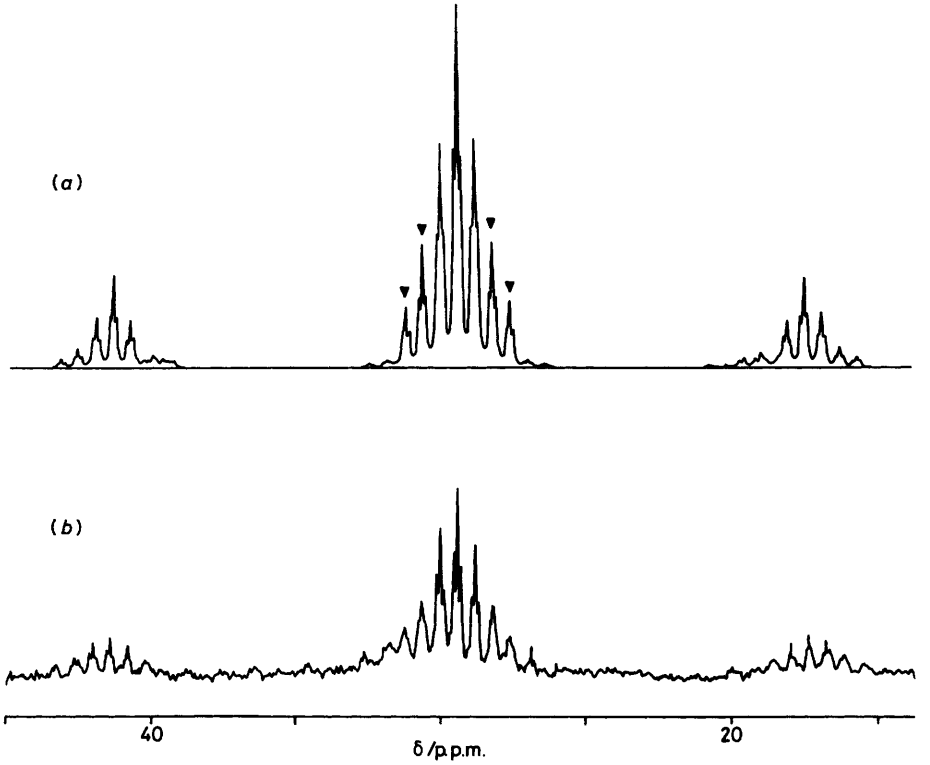

FIGURE 6 ^{31}P-{^1H} N.m.r. resonance due to the unique PPh_3 group, P^1 (Figure 7), in $[Pt_3(PPh_3)_3(\mu\text{-}PPh_2)_2(\mu\text{-}H)]^+$. Key as in Figure 5

* At 145.8 MHz, chemical shift anisotropy relaxation [16] accounts for some peaks in the observed spectrum being broadened; this broadening arises from all phosphorus couplings to either Pt^2 or Pt^3. At 45 MHz, these lines become sharp but the reduced signal-to-noise prevented us from obtaining a complete spectral analysis at this lower frequency.

from the Pt–Pt bond (2.638 Å) associated with this coupling being much shorter than the chloro-bridged Pd–Pd bond (2.89 Å) and serves to emphasize the dependence of ^3J(P–P) on the nature of the metal–metal bond in this kind of compound. It should also be noted

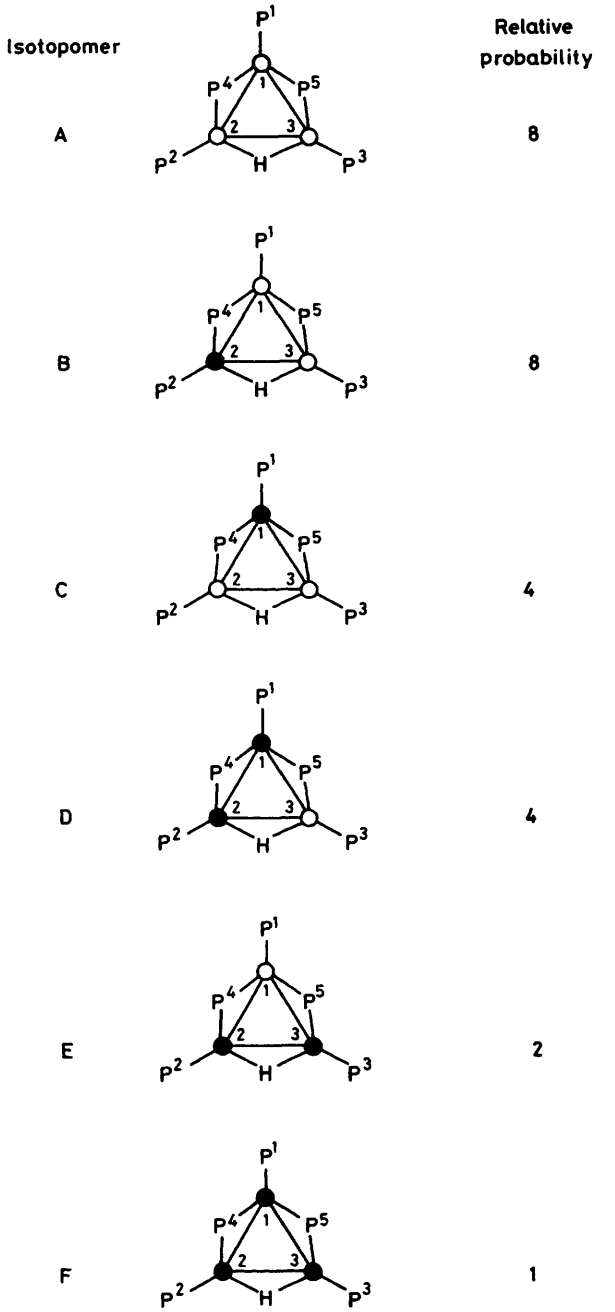

FIGURE 7 Isotopomers and their relative abundances for $[Pt_x^{195}Pt_{3-x}(PPh_3)_3(\mu\text{-}PPh_2)_3(\mu\text{-}H)]^+$ (x = 0—3). ● = ^{195}Pt, 33.8% abundant

that ^2J(P–P) is only significant for P^4 and P^5. This results from their approximate *trans*-disposition [P^{4}Pt-P^5 156.1(1)°] with all other PPtP angles being considerably less than 180° and, as demonstrated recently for a series of phosphido-bridged binuclear compounds, this angle is extremely important in determining the magnitude of ^2J(P–P).[17]

When the ^{31}P n.m.r. spectrum of (1) was recorded without ^{1}H decoupling, a further doublet splitting of the central P^{4,5} resonance resulting from isotopomer A became particularly evident [^2J(H–P^{4,5}) 55 Hz], as shown

TABLE 4

^{31}P N.m.r. data for $[Pt_3(PPh_3)_3(\mu\text{-}PPh_2)_2(\mu\text{-}H)][BF_4]\cdot 2CH_2Cl_2$ [a]

Type of phosphorus [b]	δ(^{31}P)	^1J(P–Pt)	^2J(P–Pt)	^2J(P–P)	^3J(P–P)
P^1	+29.9	3 518	358	17.6	86
P^{2,3}	+61.9	3 940	258 [c] / −120	*ca.* 0	160
P^{4,5}	+227.0	1 980 [c] / 2 500	3	260	*ca.* 0

Chemical shifts are in p.p.m. relative to external 85% H_3PO_4 as standard, coupling constants in Hz (±2.8). ^2J(H–P) of the hydride atom with the ^{31}P of the phosphido-groups (P^{4,5}) is 55 Hz, while ^1J(Pt–Pt) may be estimated to be *ca.* 2 000 Hz. [b] Numbering follows Figure 7. [c] Unique platinum atom, Pt^1.

in Figure 4(*c*). This further splitting is clearly consistent with the presence of a hydride ligand bridging the shortest Pt–Pt edge, thus maintaining the C_{2v} symmetry of the isotopomers A—E which is necessary for the n.m.r. simulation. The magnitude of ^2J(H–P^{4,5}) is also consistent with such a co-ordination site since it has recently been found for bridging hydrides in $[Ir_2(dppp)_2H_5]^+$ and $[Ir_3(dppp)_3H_7]^{2+}$ [dppp = $Ph_2P(CH_2)_3PPh_2$] [18] that ^2J(P–H$_{trans}$) is greater than ^2J(P–H$_{cis}$) with ^2J(P–H$_{trans}$) falling in the range of 60—70 Hz which is close to that found (55 Hz) in (1).

Although P–C bond cleavage in triphenylphosphine by transition metals to give a PPh_2-bridged metal cluster is not surprising,[1] (1) represents, to our knowledge, the first example of a cationic metal cluster containing both bridging hydride and phosphide groups.

We thank C.N.R. and S.E.R.C. for supporting this work and Dr. I. H. Sadler (Edinburgh University) for obtaining the ^{31}P n.m.r. spectra.

[2/011 *Received*, 5*th January*, 1982]

REFERENCES

[1] N. J. Taylor, P. C. Chieh, and A. J. Carty, *J. Chem. Soc., Chem. Commun.*, 1975, 448.
[2] D. C. Moody and R. R. Ryan, *Inorg. Chem.*, 1977, **16**, 1052.
[3] K. R. Dixon and A. D. Rattray, *Inorg. Chem.*, 1978, **17**, 1099.
[4] S. J. Cartwright, K. R. Dixon, and A. D. Rattray, *Inorg. Chem.*, 1980, **19**, 1120.
[5] D. G Evans, G. R. Hughes, D. M. P. Mingos, J. M. Bassett, and A. J. Welch, *J. Chem. Soc., Chem. Commun.*, 1980, 1255.
[6] D. E. Berry and K. R. Dixon, Roy. Soc. Chem. Meeting, Bristol, 12—24th July 1981, F6.
[7] D. M. Blake and L. M. Leung, *Inorg. Chem.*, 1972, **11**, 2879.
[8] P. L. Bellon, S. Cenini, F. Demartin, M. Manassero, M. Pizzotti, and F. Porta, *J. Chem. Soc., Dalton Trans.*, 1980, 2067.
[9] D. T. Cromer and G. B. Mann, *Acta Crystallogr.*, 1968, **12**, 321.
[10] J. B. Forsyth and M. Wells, *Acta Crystallogr., Sect. A*, 1971, **24**, 1973.

[11] ' International Tables for X-Ray Crystallography,' Kynoch Press, Birmingham, 1962, vol. 3.
[12] J. A. Ibers and D. T. Cromer, *Acta Crystallogr.*, 1958, **11**, 794; S. J. LaPlaca and J. A. Ibers, *ibid.*, 1965, **18**, 511; R. J. Doedens, W. T. Robinson, and J. A. Ibers, *J. Am. Chem. Soc.*, 1967, **89**, 4323.
[13] M. Green, J. A. K. Howard, M. Murray, J. L. Spencer, and F. G. A. Stone, *J. Chem. Soc., Dalton Trans.*, 1977, 1509.
[14] A. Albinati, *Inorg. Chim. Acta*, 1977, **22**, L31.
[15] A. Albinati, G. Carturan, and A. Musco, *Inorg. Chim. Acta*, 1976, **16**, L3.
[16] J.-Y. Lallemand, J. Soulié, and J.-C. Chattard, *J. Chem. Soc., Chem. Commun.*, 1980, 436.
[17] J. B. Brandon and K. R. Dixon, *Can. J. Chem.*, 1981, **59**, 1188.
[18] H. H. Wang and L. H. Pignolet, *Inorg. Chem.*, 1980, **19**, 1470.